Electronic Supplementary Material (ESI) for RSC Advances.

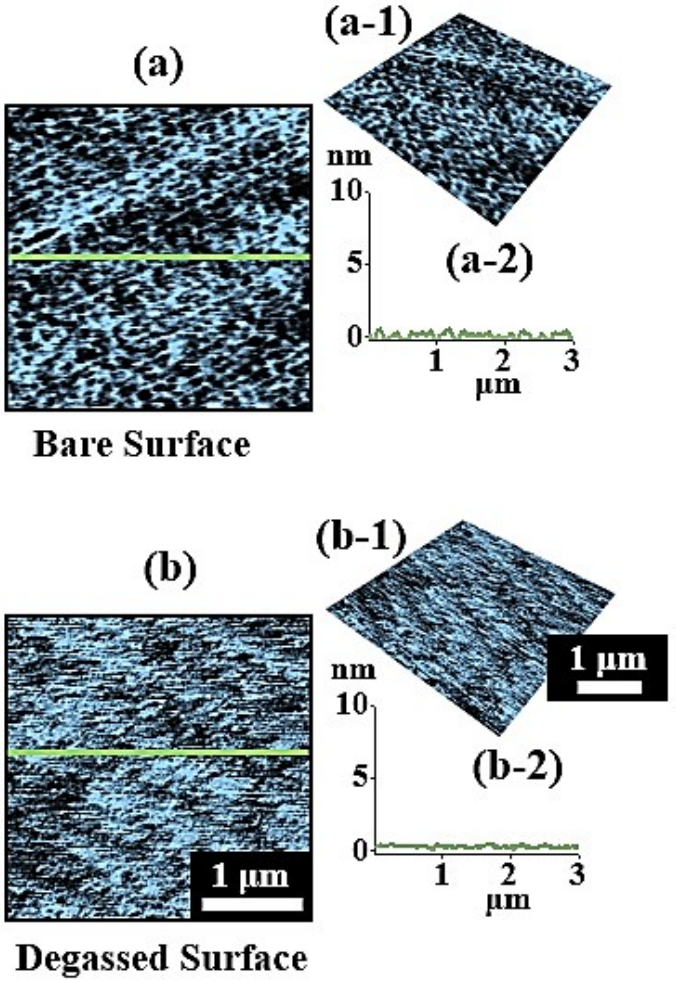

Fig. S1 (a) Bare Al_2O_3 (0001) surface. (b) Surface morphology after degassing at 350 ^oC for 1800 s. (a) - (b) AFM top views of 3 × 3 μm^2. (a-1) – (b-1) AFM side views of 3 × 3 μm^2. (a-2) – (b-2) Cross-sectional surface line profiles acquired from the green lines.

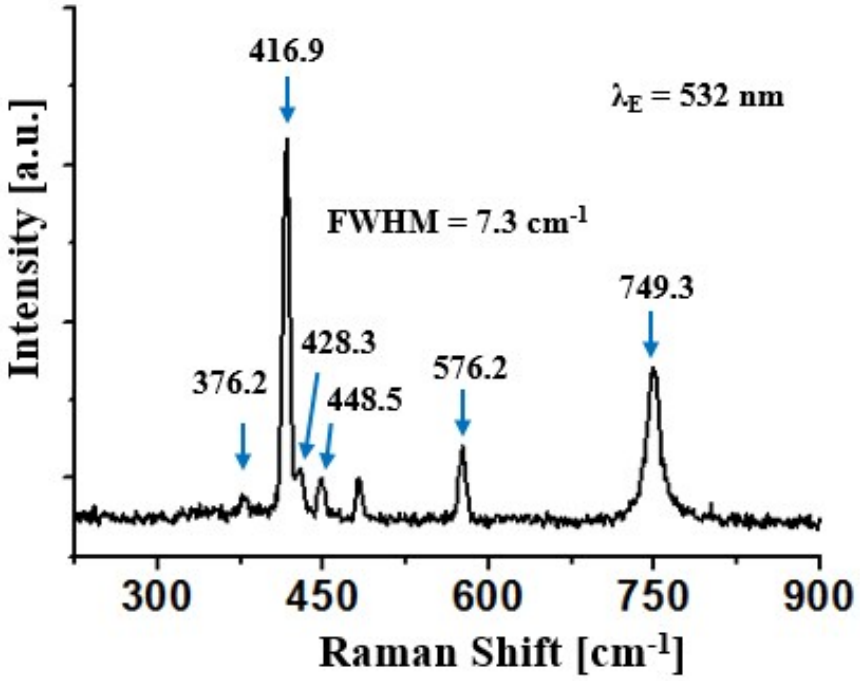

Fig. S2 Raman spectra of sapphire (Al_2O_3) (0001) substrate measured at room temperature between 225 and 900 cm^{-1}. In total 6 sapphire peaks were observed which are indicated by arrows at 376.2, 416.9, 428.3, 448.5, 576.2 and 749.3 cm^{-1}. The Raman peaks located at 376.2 and 428.3 correspond to the transverse optical (TO) modes while other peaks at 448.5, 576.2 and 749.3 are longitudinal optical (LO) modes. The peak at 416.9 is the most intense Raman active peak. The observed Raman spectra of sapphire is approximately correspond with the previous study.[1,2]

References:

1 S. Kumari and A. Khare, *Applied Surface Science*, 2013, **265**, 180-186.

2 C. C. Kuo, W. R. Liu, W. F. Hsieh, C. H. Hsu, H. C. Hsu and L. C. Chen, *Appl. Phys. Lett.*, 2009, **95**, 011905-011905.

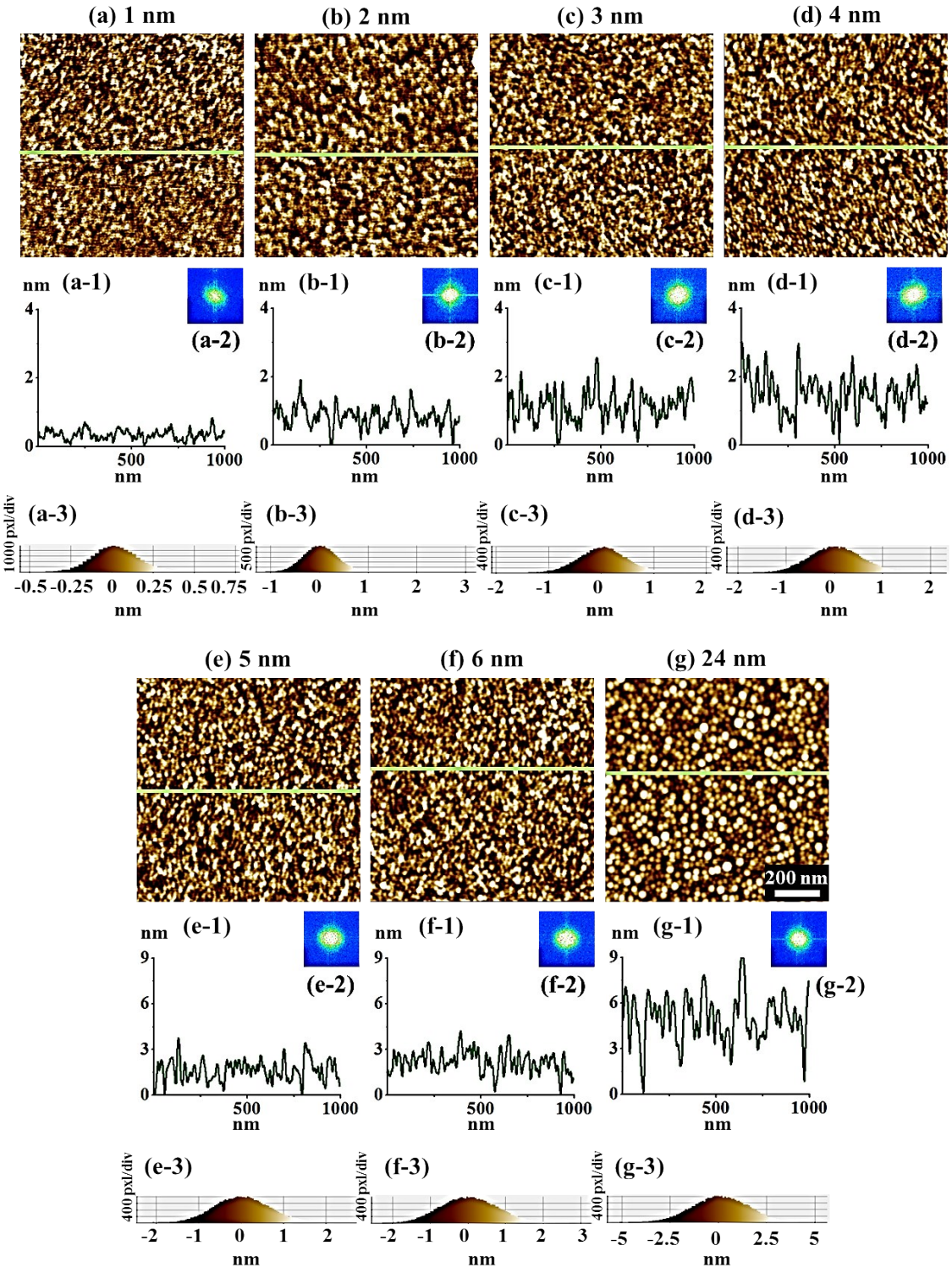

Fig. S3 Surface morphology after various Au deposition thickness between 1 and 24 nm on sapphire (0001). (a) – (g) AFM top-views of 1×1 μm^2. (a-1) – (g-1) Cross-section surface line profiles acquired from green lines in AFM top-views. (a-2) – (g-2) FFT power spectra. (a-3) – (g-3) Height distribution histogram.

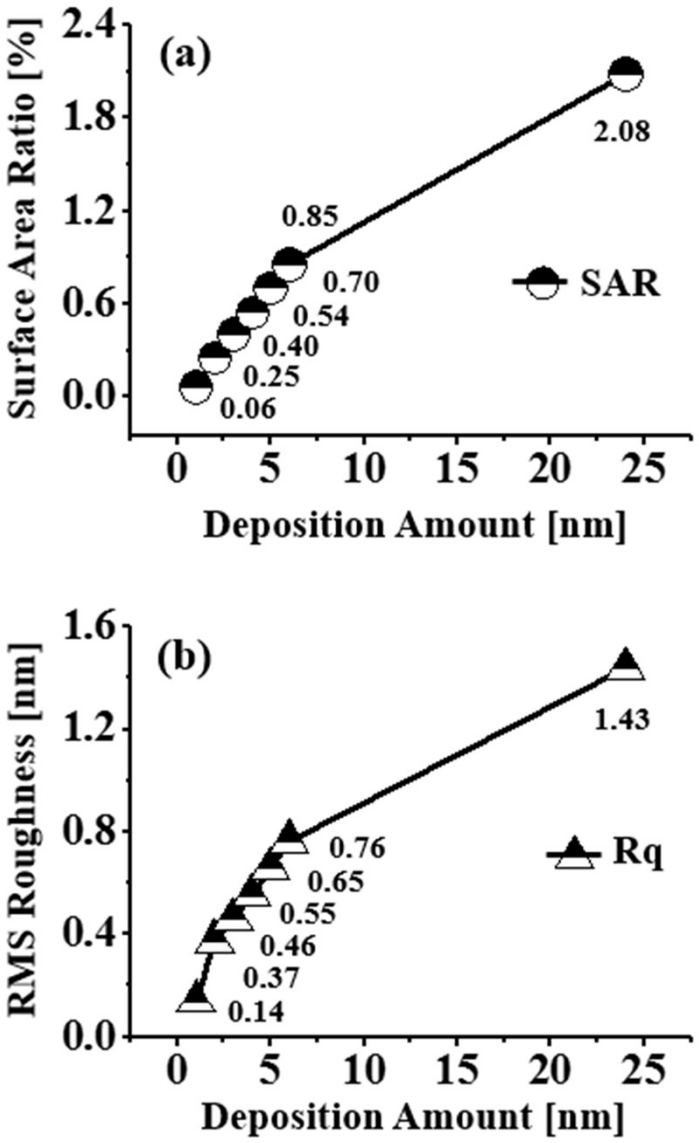

Fig. S4 Plots of (a) surface area ratio (SAR) and (b) RMS roughness (Rq) with various amount of Au deposition between 1 and 24 nm on sapphire (0001).

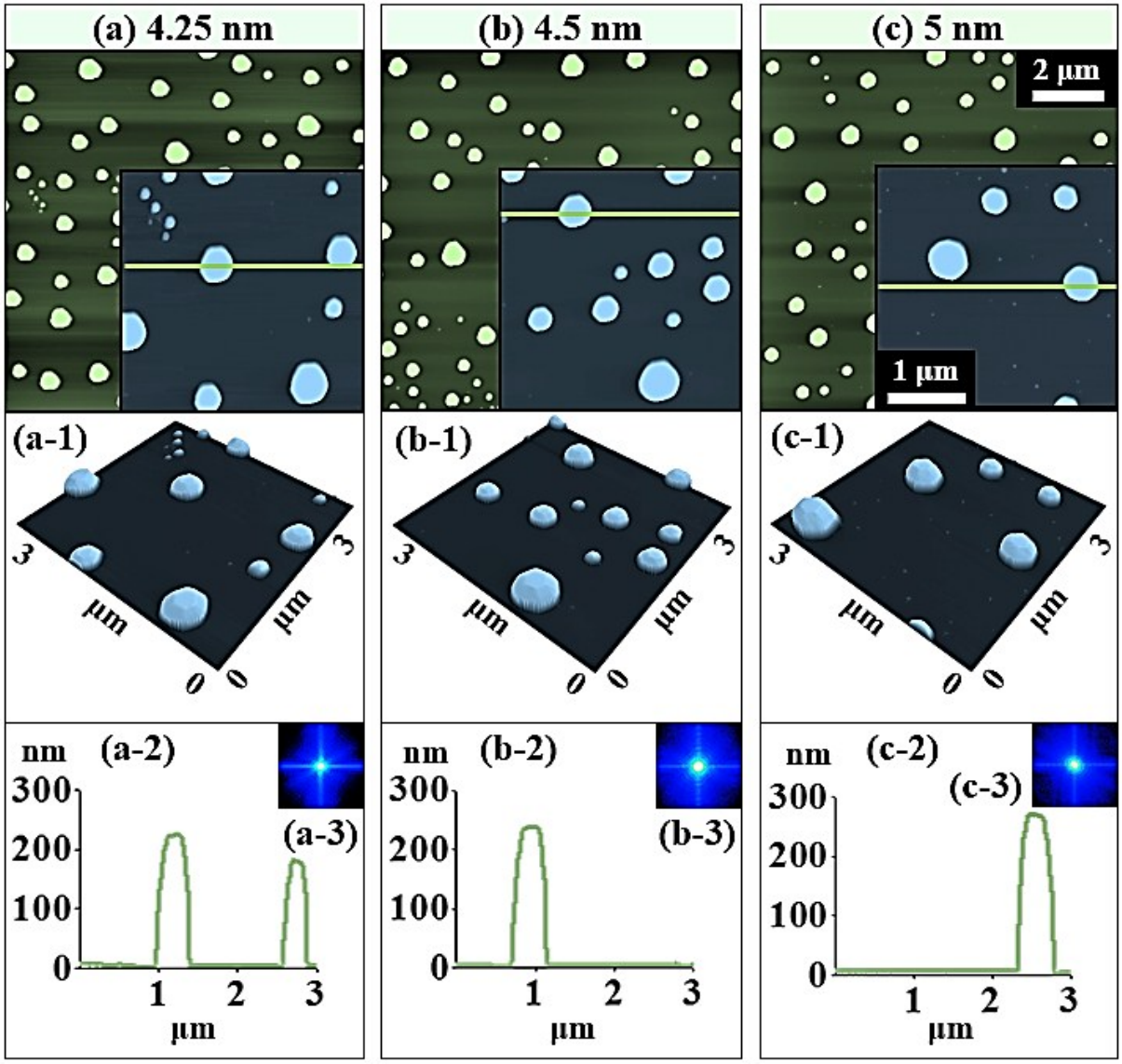

Fig. S5 Truncated Hexagonal Pyramid shape self-assembled Au NPs on Al_2O_3 (0001) between 4.25 and 5 nm of Au thickness at annealing temperature and duration of 1000 ^{o}C for 450 s. (a) – (c) AFM top views of 10 × 10 µm^2 with small scale top views of 3 × 3 µm^2. (a-1) – (c-1) AFM side views of 3 × 3 µm^2. (a-2) – (c-2) Cross-sectional line profile obtained from the green lines. (a-3) – (c-3) FFT power spectra.

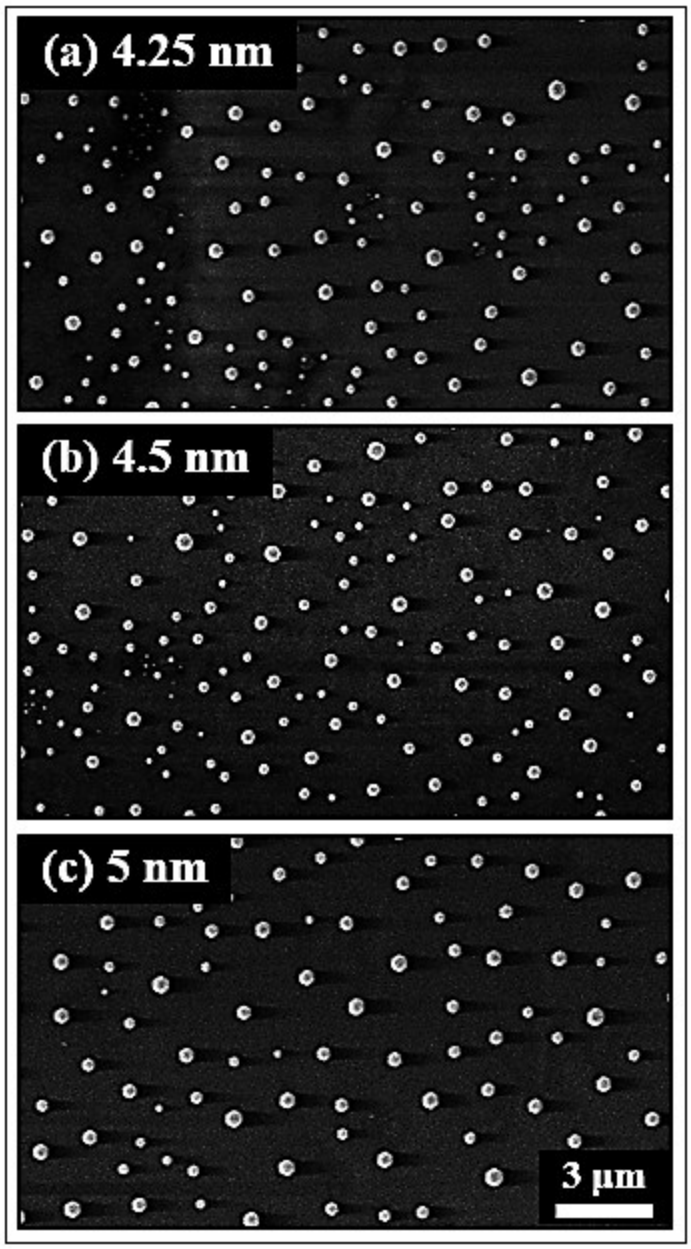

Fig. S6 Scanning electron microscopy (SEM) images of truncated hexagonal pyramid shape self-assembled Au NPs on Al_2O_3 (0001) with (a) 4.25, (b) 4.5 and (c) 5 nm of Au deposition. (a) – (c) are of 20(x) × 12(y) μm^2.

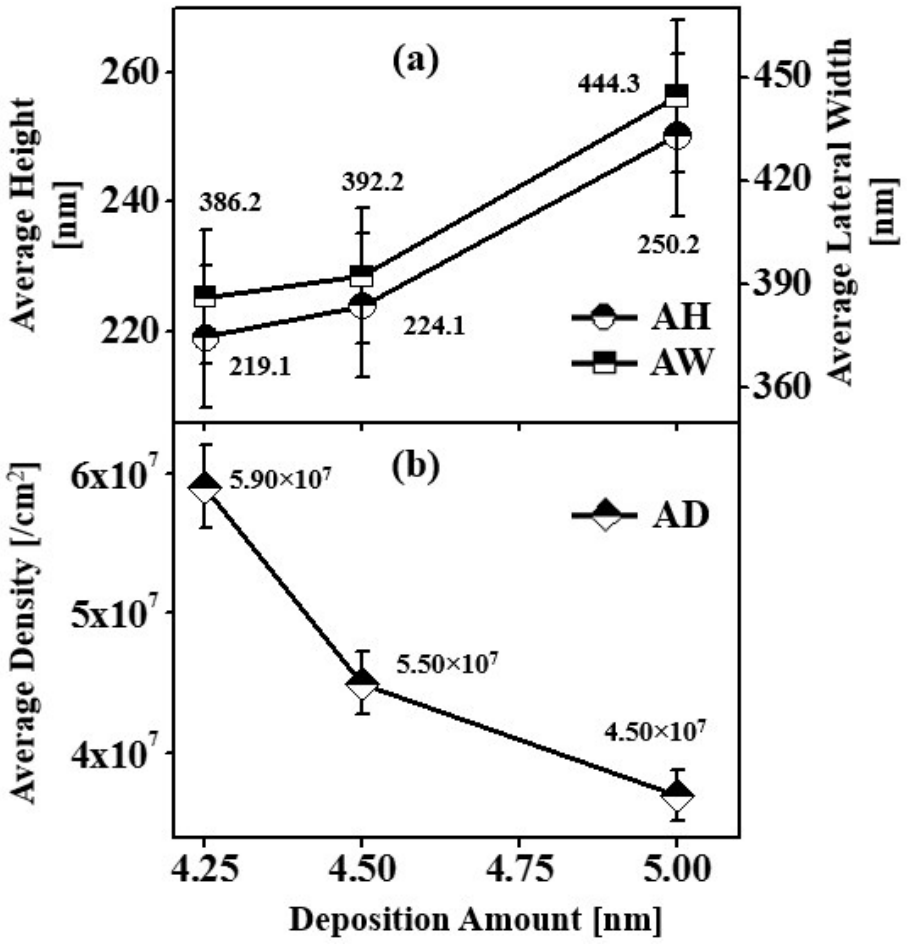

Fig. S7 Plots of (a) average height (AH) and average lateral width (AW), and (b) average density (AD) of self-assembled Au NPs fabricated on Al_2O_3 (0001) with various deposition amount. Error bars: ± 5 %.

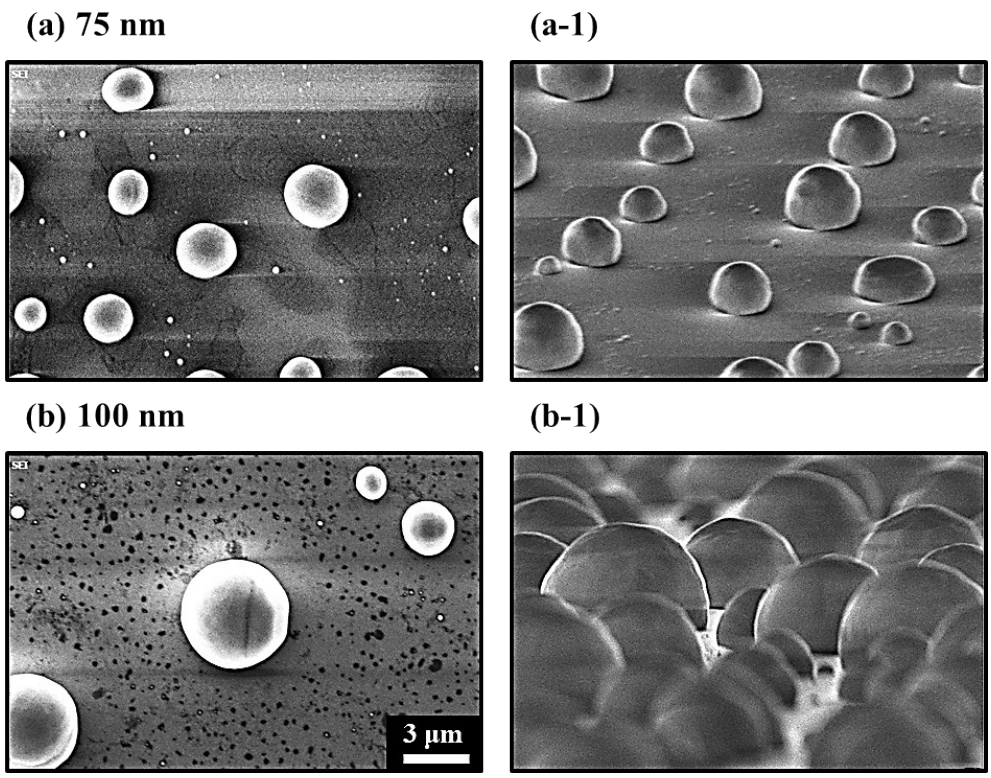

Fig. S8 SEM images of Au nanoparticles fabricated with 75 and 100 nm of Au deposition on Al_2O_3 (0001). (a) – (b) SEM top-views. (a-1) – (b-1) SEM side-views of corresponding samples. The tilt angle for the side-view (a-1) is 70^o whereas the side-view (b-1) is 90^o so the number of NPs in side-views are comparatively higher than top-views.

Table S1 Growth environment of Au nanoparticles (NPs) on Al_2O_3 (0001) with the variation of Au thickness at fixed other relevant parameters.

Sample	Degassing Temperature [^{o}C]	Degassing Duration [s]	Au deposition [nm]	Annealing Temperature [^{o}C]	Annealing Duration [s]	Growth Pressure [Torr]
1	350	1800	0.5	1000	450	1×10^{-4}
2	350	1800	1	1000	450	1×10^{-4}
3	350	1800	2	1000	450	1×10^{-4}
4	350	1800	3	1000	450	1×10^{-4}
5	350	1800	4	1000	450	1×10^{-4}
6	350	1800	4.25	1000	450	1×10^{-4}
7	350	1800	4.5	1000	450	1×10^{-4}
8	350	1800	5	1000	450	1×10^{-4}
9	350	1800	12	1000	450	1×10^{-4}
10	350	1800	24	1000	450	1×10^{-4}
11	350	1800	30	1000	450	1×10^{-4}
12	350	1800	45	1000	450	1×10^{-4}
13	350	1800	55	1000	450	1×10^{-4}
14	350	1800	75	1000	450	1×10^{-4}
15	350	1800	100	1000	450	1×10^{-4}

Table S2 Summary of average height (AH), average lateral width (LW) and average density (AD) of self-assembled Au NPs on Al_2O_3 (0001) with various deposition amount. Error Bars: ± 5 %.

Deposition Amount [nm]	**Average Height [nm]**	**Lateral Width [nm]**	**Average Density [$\times 10^7$/cm^2]**
3	47.2	102.7	1020
4	80.9	150.2	191.1
4.25	219.1	386.2	5.9
4.5	224.1	392.2	5.5
5	250.2	444.3	4.5
24	630.9	1168.2	1.3
55	751.1	2539.8	0.77
75	1475.8	3609.1	0.14
100	2591.5	6150.1	0.056